Artikel: Heavy mineral provinces as a tool for palaeogeographic reconstruction : a case study from the Buntsandstein of Nurra (NW Sardinia, Italy)

Autor: Sciunnach, Dario

DOI: https://doi.org/10.5169/seals-168889

0012-9402/01/020197-15 $1.50 + 0.20/0
Birkhäuser Verlag, Basel, 2001

Eclogae geol. Helv. 94 (2001) 197–211

Heavy mineral provinces as a tool for palaeogeographic reconstruction: A case study from the Buntsandstein of Nurra (NW Sardinia, Italy)

DARIO SCIUNNACH[1]

Keywords: sedimentology, heavy mineral provinces, palaeogeography, Hercynian Europe, Permian, Triassic

ABSTRACT

In the Nurra region, mid-Permian to Anisian red beds, commonly referred to as "Verrucano Sardo", are exposed. In the two main outcrop areas (Torre del Porticciolo and Monte Santa Giusta), however, stratigraphic sections strongly differ as to thickness, lithofacies and sandstone detrital modes. In order to better understand the relationships between the two outcrop areas, a study on the heavy mineral (HM) suites of the roughly coeval upper part of both stratigraphic sections, underlying Middle Triassic carbonates, has been carried out. For this part of the clastic succession, the name "Buntsandstein" seems more appropriate than "Verrucano Sardo".

The HM suites of the studied sandstones comprise dominantly tourmaline, zircon and rutile, along with variable amounts of apatite, garnet, chloritoid, staurolite, epidotes, amphiboles, pyroxenes, monazite and sphene; other HMs, such as spinel, andalusite, xenotime, dumortierite, vesuvianite, anatase and brookite are very minor, whereas detrital phyllosilicates (biotite, muscovite and chlorite) are widespread. Authigenic baryte and dolomite are the most abundant transparent HMs in some samples, and hydrous Mn-oxides (largely romanechite) locally dominate the opaque suite. In the Torre del Porticciolo province, the HM composition is consistent with provenance from prevailing volcanic and subordinate basement (intrusive to metamorphic) rocks, with abundant recycled detritus from older sediments. By contrast, in the Monte Santa Giusta province the HMs were sourced essentially from metamorphic and intrusive basement rocks, with lesser contribution from volcanic and sedimentary successions.

Facies characters, palaeocurrent indicators and regional data suggest that the Torre del Porticciolo clastics were deposited in a large alluvial system fed from the north; the Monte Santa Giusta clastics, instead, are better restored to a distinct alluvial fan, mostly deriving first-cycle basement detritus from the nearby medium-grade (garnet-staurolite zones) Variscan metamorphics.

Locally abundant authigenic hydrous Mn-oxides, formed as a result of sediment weathering in climatic conditions favourable to lateritisation, are consistent with tropical palaeolatitudes indicated for Sardinia at Early Triassic times in recent palaeogeographic reconstructions and support the idea of seasonal rainfall in a generally semiarid climatic context.

RIASSUNTO

Nella Nurra affiorano strati rossi di età compresa tra il Permiano Medio e l'Anisico, comunemente descritti come "Verrucano Sardo". Nelle due principali aree di affioramento (Torre del Porticciolo e Monte Santa Giusta), tuttavia, le sezioni stratigrafiche differiscono marcatamente per spessore, litofacies e mode detritiche. Per meglio comprendere i rapporti tra queste due aree, è stato condotto uno studio sui minerali pesanti (HM) delle parti sommitali – grossolanamente isocrone – di entrambe le sezioni stratigrafiche, cui si sovrappongono carbonati del Triassico Medio. Per questa parte della successione clastica, il nome "Buntsandstein" appare più appropriato di "Verrucano Sardo". L'associazione a HM delle arenarie studiate comprende prevalenti tormalina, zircone e rutilo, oltre a quantità variabili di apatite, granato, cloritoide, staurolite, epidoto, anfibolo, pirosseno, monazite e titanite; altri HM, come spinello, andalusite, xenotimo, dumortierite, vesuviana, anatasio e brookite sono assai subordinati, mentre i fillosilicati detritici (biotite, muscovite e clorite) sono diffusi. Barite e dolomite autigene sono gli HM trasparenti più abbondanti in alcuni campioni, mentre gli ossidi di Mn idrati (in genere romanechite) dominano localmente la frazione opaca. Nella provincia di Torre del Porticciolo, la composizione degli HM è compatibile con una provenienza da rocce prevalentemente vulcaniche e subordinatamente intrusive e metamorfiche, con abbondanti apporti di detrito riciclato. Al contrario, nella provincia di Monte Santa Giusta gli HM derivano essenzialmente da rocce metamorfiche e intrusive, con minori contributi da successioni vulcaniche e sedimentarie.

I caratteri di facies, gli indicatori di paleocorrenti e il quadro regionale suggeriscono che i clastici di Torre del Porticciolo si siano deposti in un ampio sistema alluvionale alimentato da nord; i clastici di Monte Santa Giusta, invece, si riconducono meglio ad una conoide alluvionale distinta, alimentata in prevalenza da detriti metamorfici di primo ciclo provenienti dal vicino basamento Varisico (zone a granato-staurolite).

Gli ossidi di Mn idrati, autigeni nel sedimento e legati ad esposizione subaerea in condizioni climatiche favorevoli alla lateritizzazione, concordano con le paleolatitudini tropicali indicate per la Sardegna all'inizio del Triassico nelle più recenti ricostruzioni paleogeografiche e avvalorano un modello di piovosità stagionale in un contesto climatico generalmente semiarido.

Introduction

Palaeogeographic reconstructions of Sardinia in the late Paleozoic have great bearing to unravelling the ancient geological scenarios of post-Variscan southern Europe. Until now, attempts at detailed reconstructions in this area have been largely hampered by the poor exposure of Permian sedimentary rocks, the scarcity of biostratigraphic checkpoints, and the disruption of the Hercynian range during the Alpine evolution of the Western Mediterranean, which since the Early Miocene

[1] Dipartimento di Scienze della Terra and CNR – Centro di Studio per la Geodinamica Alpina e Quaternaria, Via Mangiagalli, 34, 20133 Milano, Italy.
Address: Struttura Analisi e Informazioni Territoriali, Regione Lombardia, Piazza Duca d'Aosta 4, 20124 Milano, Italy.
E-mail: Dario_Sciunnach@regione.lombardia.it

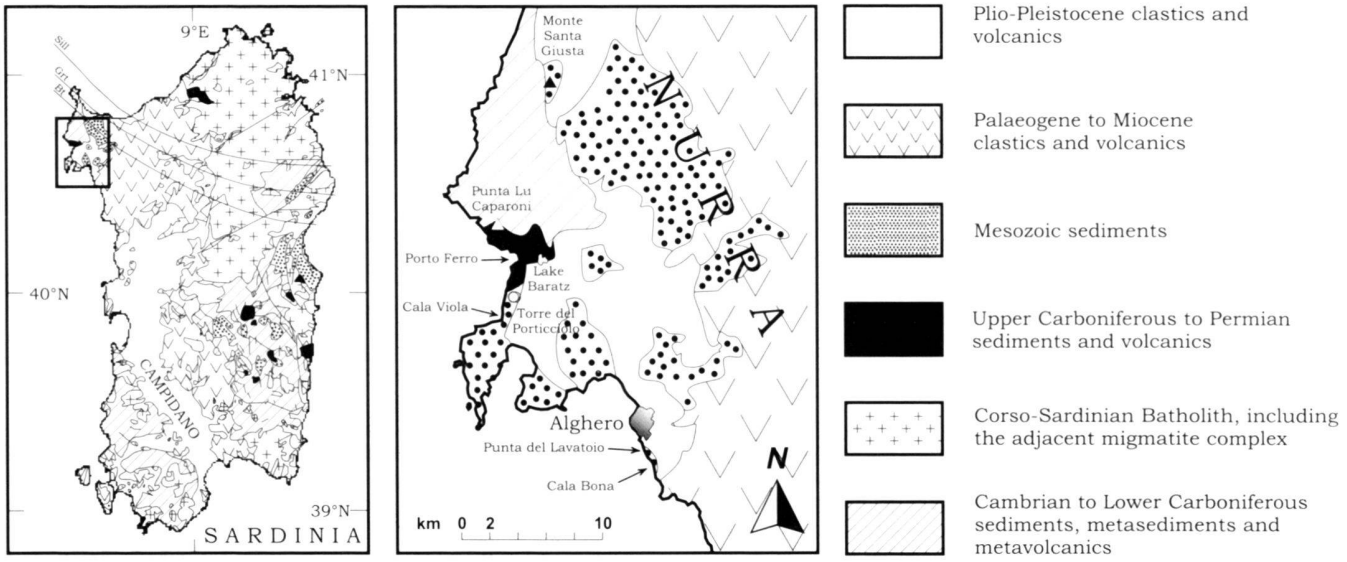

Fig. 1. Geological sketch map of the study area. Main isograde of the Hercynian metamorphism, corresponding to the southern boundaries of the biotite (Bt), garnet (Grt) and sillimanite (Sill) zones are also drawn after Ghezzo & Orsini (1982). For a detailed location of single outcrops of the Permian-Triassic clastic succession of Nurra, as well as of the boreholes drilled into it, the reader is referred to fig. 1 of Gasperi & Gelmini (1979).

has rotated the Corso-Sardinian Block counterclockwise with respect to stable Europe.

At the end of the Paleozoic, Sardinia was a part of the Hercynian orogen, facing present-day Provence and Languedoc (Westphal et al. 1976): pre-Variscan rocks, essentially hemipelagites and turbidites, had been metamorphosed up to the sillimanite zone at the contact with the Corso-Sardinian Batholith, one of the largest in Europe. Palaeolatitudes were equatorial to tropical, and the island was located close to the continental platform bordering the western edge of the Tethys Ocean (Golonka et al. 1994). Post-orogenic clastic sedimentation in a continental setting started in the Westphalian (Fontana et al. 1982) but was confined to small fault-bounded basins up to Saxonian ~ Kungurian times (Broutin et al. 1994). Intercalations of intermediate to acidic volcanics (thick rhyolitic ignimbrites, andesitic to rhyolitic lava flows and thin tuffaceous layers) occur at various levels in the Permian succession, documenting post-orogenic magmatism coeval with sedimentation over a time span possibly exceeding 20 Ma.

In the Nurra region (Fig. 1), Lower Permian clastics (Punta Lu Caparoni Fm.: Gasperi & Gelmini 1979) occur as small, scattered outcrops, whereas mid-Permian to Anisian clastics are better exposed in two distinct outcrop areas, where, however, they display strongly different thickness, lithofacies and sandstone detrital modes. The main outcrop area is found along the shore of the Sardinia Sea, from Porto Ferro (Fig. 2a) to Cala Viola near the Torre del Porticciolo village (Fig. 2b), and extends southwards as far as Cala Bona near Alghero. The second significant outcrop area is located in central Nurra, at Monte Santa Giusta (actually a hillock, just 251 m a.s.l.; Fig. 2c). Data from coal exploration boreholes (Lotti 1931) are useful to constrain thickness and stratigraphy of the clastic succession. Correlation of the two main outcrop areas is regarded as still unclear and needing further investigation (Cassinis et al. 1996).

In the present paper, sedimentological observations and quantitative heavy mineral data from these considered successions, when in the framework of the available regional and stratigraphic information, shed new light on the relationships between the two outcrop areas and on their palaeogeographic significance.

Regional Framework

Crystalline basement

In the study area (central to southern Nurra; Fig. 1) Variscan metamorphics mostly consist of low-grade sericite and quartz phyllites enclosing quartz rods and tiny carbonaceous seams. Colour ranges from grey-greenish to almost black; slaty and crenulation cleavages are conspicuous in outcrop. Typical parageneses, belonging to the chlorite zone, comprise quartz, albite, muscovite, chlorite, chloritoid, paragonite, metamorphic vermiculite, carbonates, graphite and ilmenite. Northwards, stepwise appearances of biotite, garnet, staurolite, kyanite and sillimanite define steep regional isograds indicating increasing Variscan metamorphic overprint from the chlorite zone, up to the sillimanite+K-feldspar zone of the amphibolite facies (Franceschelli et al. 1982) at the margin of the Corso-Sardinian batholith, where both calc-alkaline and anatectic magmatic products are widely represented (Ghezzo & Orsini 1982).

Age of the protoliths is largely considered as Early to mid-Paleozoic; deformation and metamorphism seemingly took

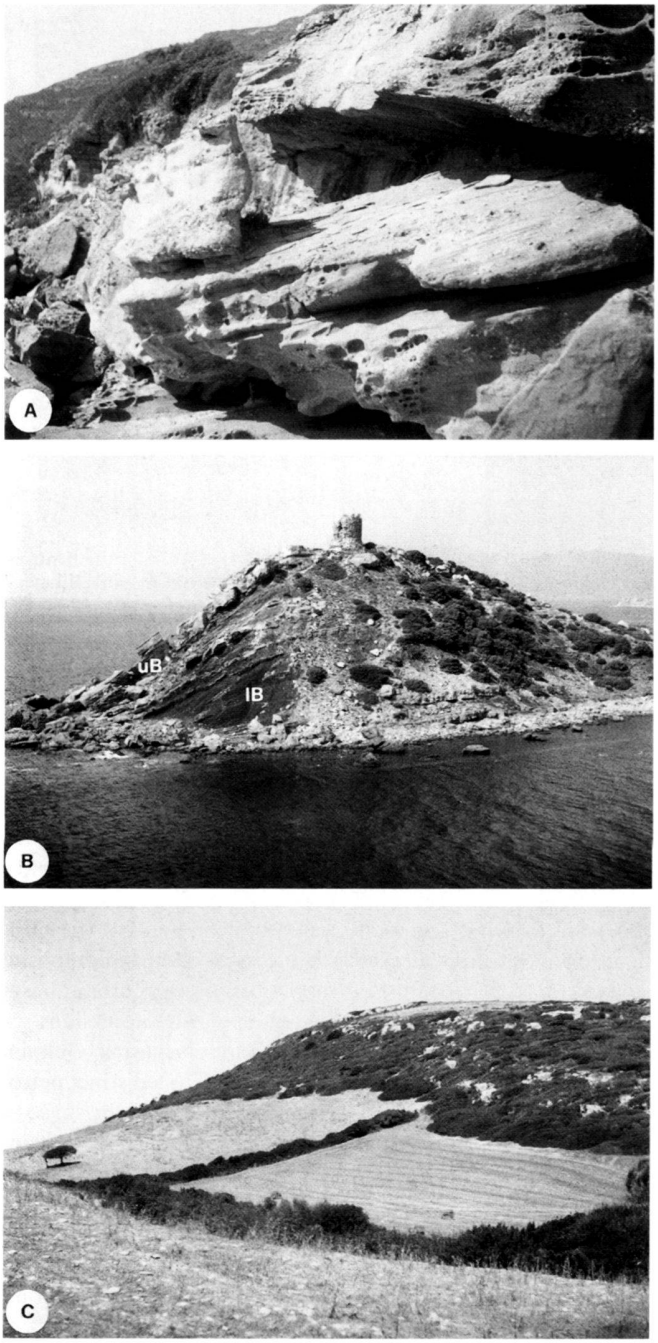

Fig. 2. Outcrop conditions of the Permian-Triassic clastic succession of Nurra. A) The Porto Ferro cliff, here about 4 m-high, where fining-upward metric cyclothems of conglomerates and sandstones with large-scale trough-bedding are exposed. B) The Torre del Porticciolo *cuesta*, where alternating sandstones and siltstones (lB) are sharply overlain by the conglomerate bank at the base of the uB. C) The Monte Santa Giusta hillock, where outcropping Middle Triassic carbonates overlie poorly exposed continental clastics.

place since the late Early Carboniferous and came to an end by Westphalian times (Franceschelli et al. 1982 and references therein), when the Variscan basement was exhumed.

Sedimentary successions

Similarities between the post-Variscan sedimentary successions of Sardinia and the classical Permo-Trias of Germany were recognised more than a century ago (Lovisato 1884; De Stefani 1891). However, above the oldest clastic deposits, unconformably overlying the metamorphic basement (Lower Rotliegend), no Zechstein evaporites are found in Sardinia. Instead, a thick clastic succession of fossil-barren red beds passes upwards to a more characteristic Buntsandstein (Vardabasso 1966). The Middle and Upper Triassic of Sardinia are widely held as displaying a typical Germanic facies, with well represented Muschelkalk carbonates and Keuper evaporites; actually, the Muschelkalk facies of mid-Carnian age in Sardinia (Carrillat et al. 1999) finds no analogue in Germany, where the Muschelkalk/Keuper boundary falls well into the Ladinian (Aigner & Bachmann 1998).

Stratigraphy. Clastic sedimentation after the Variscan metamorphism began in north-western Sardinia with lacustrine fanglomerates to mudrocks, up to 15 m-thick (Punta Lu Caparoni Formation: Gasperi & Gelmini 1979) overlain by alluvial red beds, up to 250 m-thick (Verrucano Sardo: Vardabasso 1966). This clastic succession was thoroughly revised in Gasperi & Gelmini (1979), where the Verrucano Sardo was distinguished from the underlying Punta Lu Caparoni Formation and subdivided into four informal units of lesser rank, numbered 1 to 4 in ascending stratigraphic order and conceptually corresponding to lithozones (Fig. 3); this subdivision, however, does not apply to the condensed section of Monte Santa Giusta. More recently, Cassinis et al. (1996) stressed similarities of the upper Verrucano Sardo (Units 3 and 4 of Gasperi & Gelmini 1979) with the Germanic Buntsandstein, and questioned the use of the name "Verrucano" for red beds deposited outside the Alpine-Apenninic type areas.

Within the whole clastic succession, the only valuable biostratigraphic data are reported from the Punta Lu Caparoni Formation, where upper Autunian (~ Artinskian) macro- and microfloral remains occur (Pecorini 1962; Broutin et al. 1996; Ronchi et al. 1998), and from the upper part of the Verrucano Sardo at Cala Viola, where abundant remains of the Triassic *Equisetum mougeotii* Brongt occur in a "white-greenish, arenaceous-shaley intercalation" in cross-bedded red sandstones, also containing *Estheria* (Pecorini 1962). At Cala Viola, the upper part of Lithozone 3 and the whole Lithozone 4 are exposed, but a greenish shale facies occurs only in the uppermost three metres of Lithozone 4; it is thus likely that the Triassic plant remains were found in the upper part of Lithozone 4, as indicated also by Vardabasso (1966), and not in Lithozone 3, as interpreted by Gasperi & Gelmini (1979). Although the *Equisetum* remains were regarded as strictly Early Triassic in age by Pecorini (1962), they might be Middle Triassic as well (R.H. Wagner, pers. comm.).

An upper boundary for the age of the clastic succession is provided by the overlying shallow-water Muschelkalk carbon-

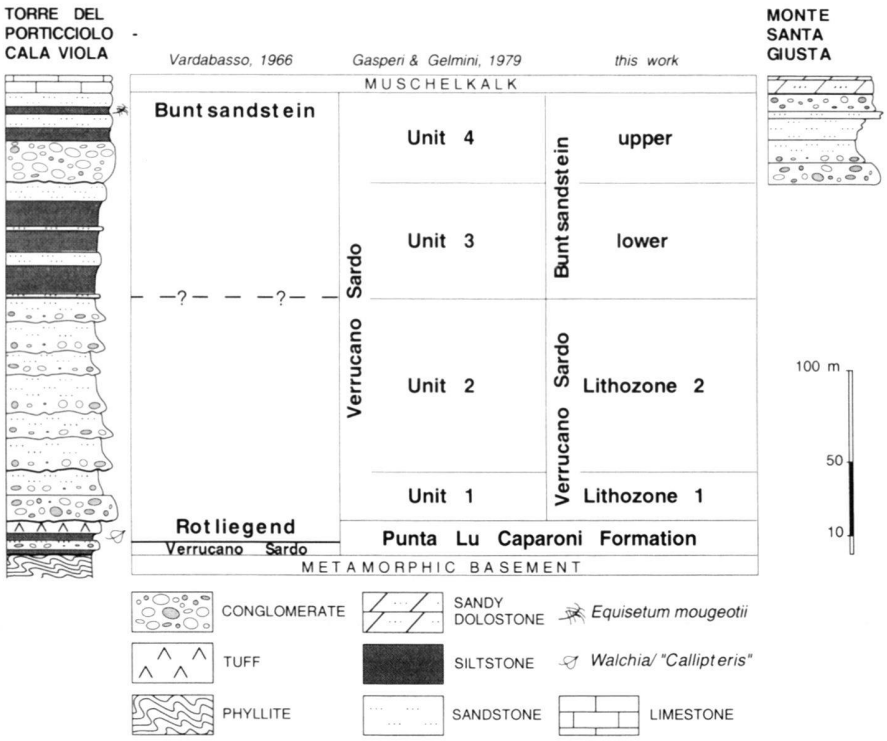

Fig. 3. Stratigraphic framework for the Permian-Triassic clastic succession of Nurra, bracketed between the Hercynian basement and the Middle Triassic transgressive carbonates in Muschelkalk facies. In Gasperi & Gelmini (1979), the Monte Santa Giusta clastic succession is correlated to Unit 2 of the Verrucano Sardo instead of Unit 4 (upper Buntsandstein).

ates (Punta del Lavatoio and Monte Santa Giusta areas; Fig. 4). In the Punta del Lavatoio section, an Early Ladinian age was established for the carbonates in the upper part, based on calcareous algae and cephalopods (Gandin 1978); to date, fossils of unequivocal biostratigraphic value have not been found in the lower part, which has been ascribed only tentatively to the Anisian according to microfloral data (Pittau Demelia & Flaviani 1982). In the Monte Santa Giusta section, lower Fassanian (lowermost Ladinian) palynomorphs have been recently obtained from the very base of the carbonate succession, along with upper Fassanian-lower Longobardian (mid-Ladinian) conodonts from the lower to middle part and upper Cordevolian-Julian (mid-Carnian) palynomorphs from the upper part (Carrillat et al. 1999).

Regarding stratigraphic position, Lithozones 1 and 2 of the Verrucano Sardo can be tentatively ascribed to the uppermost Lower to Upper Permian (Kungurian to Lopingian). A relative sea-level rise is documented, beginning at the base of Lithozone 3, by encroachment of Buntsandstein-like deltaic facies onto a high-energy continental braidplain (see discussion below). This may correspond to the major eustatic rise at the onset of the Triassic (Sequence UAA-1.2 of Haq et al. 1987; Holser & Magaritz 1987). If so, Lithozone 3 should represent most of the Lower Triassic and Lithozone 4 at least part of the Anisian.

In the present paper, Lithozones 3 and 4 of the Verrucano Sardo will be termed lower and upper Buntsandstein (lB and uB), respectively. The following data concern the mid-Permian to Triassic clastic succession. The Punta Lu Caparoni Formation is beyond the scope of the present paper.

Sandstone petrography. The Verrucano Sardo sandstones of the Torre del Porticciolo area, best exposed in the Porto Ferro-Cala Viola section, can be classified as volcanic arenites to sublitharenites (Folk 1974) depending on quartz content; they invariably fall in the "recycled orogen" field of the QFL diagram of Dickinson (1985) (Fig. 5), reflecting composite source areas that comprised metamorphic to plutonic basement rocks as well as volcanic and older clastic successions.

Each of the four units established by Gasperi & Gelmini (1979) (Fig. 3) corresponds remarkably well to a distinct petrologic interval (Ronchi 1993; Cassinis et al. 1996) in the sense of Dickinson & Rich (1972), that is, to a definite stratigraphic interval characterised by a distinctive sandstone composition (petrofacies; Tab. 1). In detail, the immature Petrofacies 1a and 1b overlap on the QFL diagram but can be distinguished by means of the C/Q and V/L ratios of Dickinson (1970), whereas the submature Petrofacies 2 (lB) marks a sharp increase in the abundance of feldspars and quartz concurrent with a sharp decrease in the abundance of volcanic lithics. Petrofacies 2 also records the first appearance of abundant interstitial carbonates (15±8% of rock volume on 10 samples: Ronchi 1993) in sandstones of the Permian-Triassic succession. The mature Petrofacies 3 (uB) marks a further and more dramatic enrichment in detrital quartz, along with depletion in volcanic lithics. Vertical evolution of detrital modes thus depicts a stepwise trend of clastic sediments towards higher mineralogical stability and textural maturity, reflecting the interplay of longer residence time in the depositional environment before burial, increasing dissection of the post-Variscan vol-

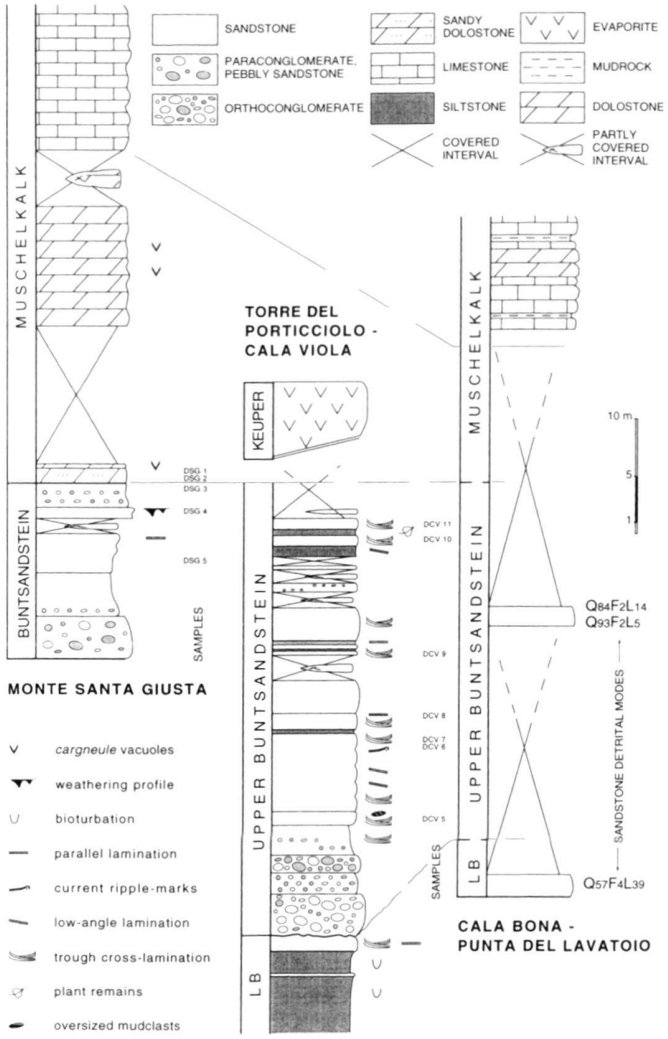

Fig. 4. Schematic stratigraphic sections and correlations around the Buntsandstein/Muschelkalk boundary.

canics along with the concurrent unroofing of quartz-rich basement rocks, and possible recycling of older sediments. All these processes are consistent with a general scenario of progressively subdued relief as the Hercynian basin-and-swell palaeotopography approached peneplanation.

The immature sandstones from Monte Santa Giusta (Petrofacies 4) range from arkoses and lithic arkoses to subarkoses, and step into the "continental block" field of the QFL diagram (Fig. 5), reflecting prevailing basement sources.

The diagenetic grade of the whole clastic succession is seemingly low (semi-mature stage of Schmidt & McDonald (1979), broadly corresponding to the epigenetic stage *sensu* Kossovskaya & Shutov (1970), as suggested by limited evidence for mechanical compaction (strained monocrystalline quartz, fractured brittle grains and kinked mica flakes are very rare), by inconspicuous growth of authigenic minerals in oversized secondary pores cross-cutting the boundaries of framework grains, and by abundance of kaolinite booklets preserved in the epimatrix.

Correlations. The Verrucano Sardo of Nurra may be broadly correlated with the Permotriassic clastic units, sparsely outcropping over a wide domain embracing central Iberia, the Balearic Islands, and Southern France (Lodève and Estérel areas); correlations with Corsica are more problematic due to the overwhelming penecontemporaneous volcanic products exposed there (Broutin et al. 1994). The diachronous onset of the Buntsandstein facies in Southern Europe, ranging from the Thuringian (~ Lopingian) in the southern Pyrenees (Broutin et al. 1988) to the Anisian in Languedoc (Broutin et al. 1994) and up to the Ladinian in the western Iberian Range (Sopeña et al. 1988), has been demonstrated through regional biostratigraphic correlation; accordingly, the underlying red bed facies is expected to be older in subsiding areas accommodating thicker sedimentary successions, and younger on structural highs inherited from the late Hercynian basin-and-swell palaeotopography. Under this respect, correlation of continental deposits based on lithofacies alone can be particularly misleading, and should be supported by more reliable correlation criteria. In the present paper, the term "Buntsandstein" is used, in fact, to identify a sediment package characterised by a distinctive facies in the field, rather than a strict chronostratigraphic equivalent of the Lower Triassic.

In the Nurra area, a datum plane is provided by the major marine transgression causing encroachment of shelfal carbonate facies onto the underlying continental to transitional clastic successions. The available biostratigraphic data constrain this

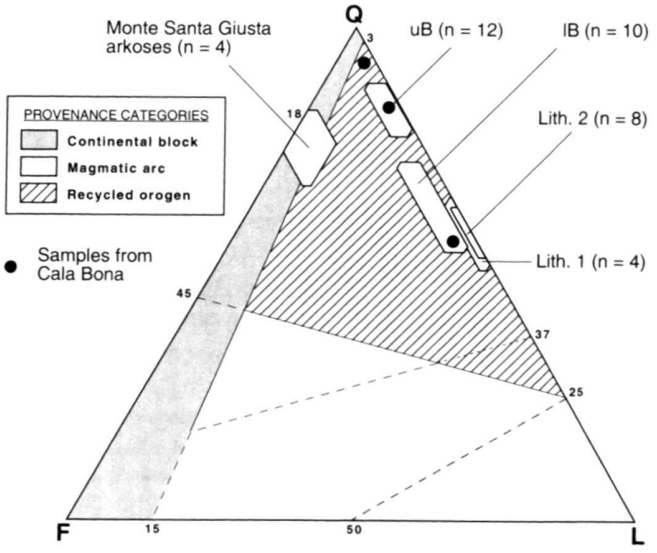

Fig. 5. Petrofacies of the Permian-Triassic sandstones of Nurra (simplified after Ronchi 1993; Cassinis et al. 1996) plotted on the QFL diagram of Dickinson (1985). Polygons are one standard deviation each side of the mean; n = number of studied samples.

VERRUCANO SARDO (Vardabasso, 1966; Gasperi & Gelmini, 1979)				Petrofacies
Lithozone 1	Q = 58.4 F = 1.0 L = 40.8	σ = 7.4 σ = 1.3 σ = 7.0	0.5 > C/Q > 0.34 V/L > 0.9	1a
Lithozone 2	Q = 58.6 F = 0.5 L = 40.1	σ = 5.1 σ = 0.8 σ = 4.8	C/Q > 0.6 V/L < 0.9 (except for the sample yielding the peak in abundance of lithic grains)	1b
Lithozone 3 (lB)	Q = 63.8 F = 4.4 L = 31.7	σ = 9.1 σ = 2.3 σ = 10.2		2
Lithozone 4 (uB)	Q = 83.4 F = 2.5 L = 14.0	σ = 5.4 σ = 2.3 σ = 6.3		3
MONTE SANTA GIUSTA ARKOSES				
	Q = 75.6 F = 20.2 L = 4.0	σ = 7.7 σ = 5.0 σ = 4.4		4

Table 1. Mean petrofacies parameters for the Permian-Triassic sandstones of Nurra (simplified after Ronchi 1993). C/Q and V/L ratios (after Dickinson 1970) are reported only where they allow discrimination of petrologic intervals (Dickinson & Rich 1972) characterised by identical QFL modes.

transgression as not younger than the early Fassanian (Gandin 1978; Carrillat et al. 1999) and probably not older than the Illyrian (TST of the 3rd order sequence UAA-2.2 of Haq et al. 1987).

Exposure conditions of the datum plane in the study area are variable (Fig. 4). At Cala Viola, the arenaceous uB passes upwards to a covered interval; adjacent, strongly deformed evaporites ascribed to the Keuper are interpreted to be in tectonic contact with the uB.

At Cala Bona, grey-greenish to pinkish sandstones, poorly exposed underneath the Quaternary marine terraces ("*panchina*"), are reliably correlated to both the lB and the uB based on sandstone facies and detrital modes (Figs. 4, 5). Above a covered interval, these clastics are in turn overlain by grey bedded limestones representing the Muschelkalk (Punta del Lavatoio section: Gandin 1978). Although the contact cannot be directly observed, Buntsandstein and Muschelkalk display the same strike and dip below and above the covered interval.

At Monte Santa Giusta, the boundary between reddish arkosic sandstones and grey bedded limestones is transitional and marked by yellowish hybrid carbonates, vuggy dolostones and *cargneules* over 25 m-thick. The overlying grey carbonates in Muschelkalk facies yielded Fassanian palynomorphs and conodonts, and therefore can be reliably ascribed to the regional Middle Triassic transgression (Carrillat et al. 1999).

Gasperi & Gelmini (1979) correlated the underlying Monte Santa Giusta arkoses with Lithozone 2 of the Verrucano Sardo (Porto Ferro section); this statement, not justified in the cited paper, possibly relies on the occurrence of volcanic intercalations, reported in both stratigraphic intervals, as well as on their similarities as to colour and pebble size. Basic concepts of stratigraphic correlation would suggest to regard the Monte Santa Giusta arkoses as largely coeval with Lithozone 4 (uB) since both stratigraphic intervals underlie shallow-water shelfal carbonates, representing the Muschelkalk transgression. The hybrid dolostones of Monte Santa Giusta might correspond, at least in part, to the covered stratigraphic interval of the Cala Bona-Punta del Lavatoio section.

Sedimentology

Lithozone 1 of the Verrucano Sardo (over 20 m-thick) consists of fining-upward cyclothems 4 to 6 metres-thick, comprising massive paraconglomerates in lenticular beds passing upwards to moderately to poorly sorted, whitish coarse-grained sandstones, arranged in amalgamated bedsets and displaying parallel and cross-bedding. Rare silty plugs, up to 50 cm-thick, locally display Mn-rich weathering crusts. Pebbles, up to 15 cm in diameter, consist of milky quartz, ignimbrite and sandstone. A proximal alluvial fan environment, incised by high-energy braided streams, is indicated: the fining-upward cyclothems are interpreted as the result of stream-floods.

Lithozone 2 (over 75 m-thick) consists of red beds arranged in metric to decametric cyclothems (Fig. 2a) commonly comprising, bottom to top:

a) channelised orthoconglomerates and pebbly sandstones, locally scouring, by up to 80 cm, the sandstones to siltstones at the top of the underlying cyclothem (Fig. 6a, b); imbricated pebbles are common, and sieve deposits locally occur. This facies corresponds to an active channel-lag.

b) moderately sorted, coarse-grained sandstones with parallel, low-angle, and trough cross-lamination; cross-bedded sandstones, downlapping at angles exceeding 30° onto pebbly channel-lags, are interpreted as channel bars (Fig. 6c).

c) deep red, fine-grained sandstones and siltstones, corresponding to the clay plugs of abandoned channels and/or to overbank marshes; these intervals, commonly thin (35 cm on the average, n = 4) with respect to the coarser grain size fractions of the cyclothem, are not always preserved.

Besides this typical fining-upward trend, inverse ("coarse-tail") grading is locally observed and tentatively interpreted as a result of temporal increase in river discharge during rising flood conditions.

The conglomerates contain prevailing subrounded to rounded pebbles of red ignimbrite, up to 20 cm in diameter, along with milky quartz (subangular pebbles up to 12 cm in diameter), metamorphic clasts ranging from greenschist to amphibolite facies (angular pebbles up to 13 cm) and rare plutonics (subrounded pebbles up to 11 cm); intraformational mudclasts are absent. Lithozone 2 represents a distal alluvial fan to high-energy braided stream environment. The fining-upward cyclothems are interpreted as the result of sheet-floods and their thickness, decreasing from about 10 m in the lower part to 1±0.5 m (n = 8) in the upper part, points to progressively more subdued relief in the drainage basin and/or to increasing aridity. Depth of the channels (42±27 cm on the average, n =

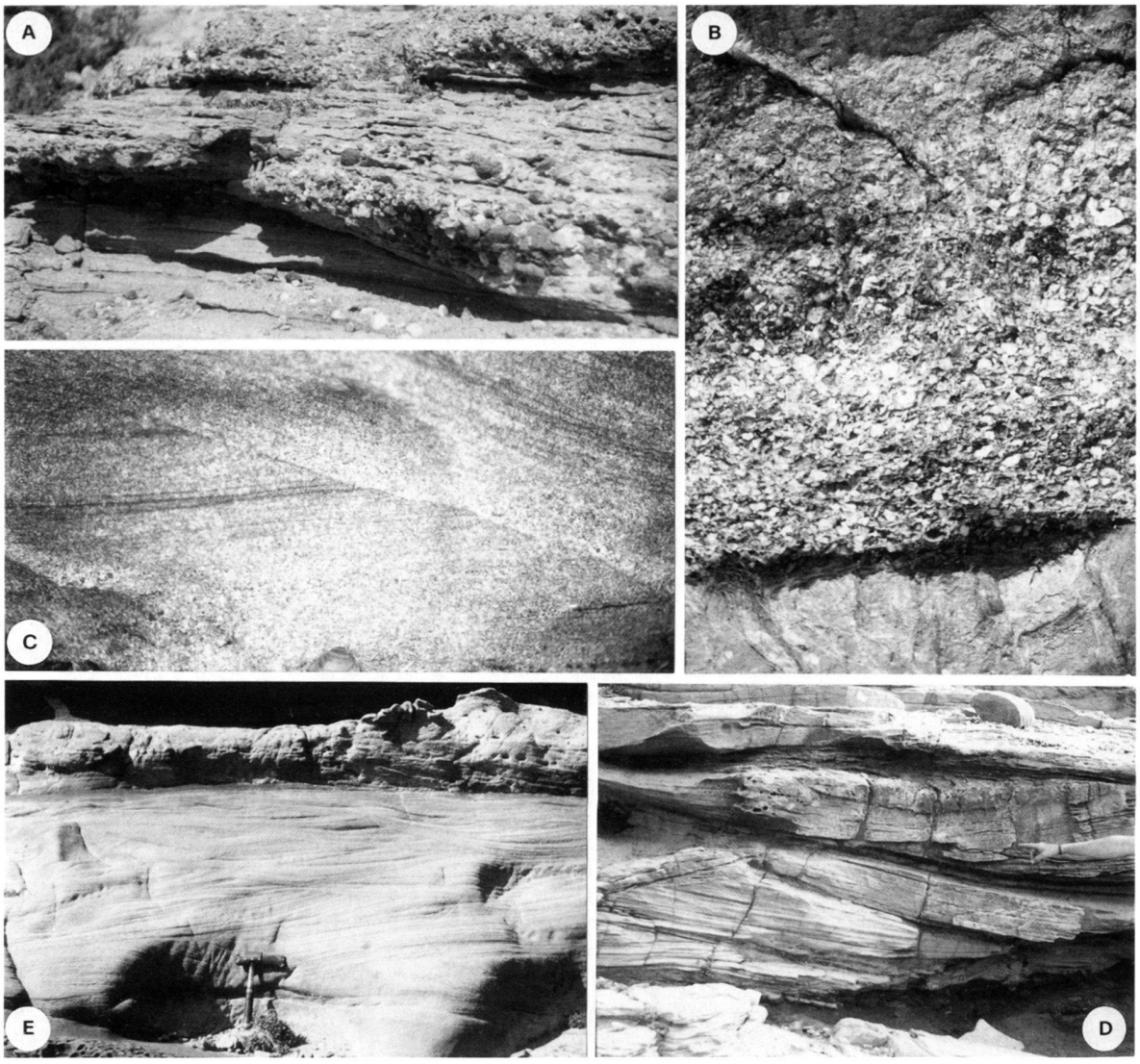

Fig. 6. Sedimentology of the mid-Permian to Triassic clastics of the Porto Ferro-Cala Viola area. A) Channel fill cyclothems, with orthoconglomerate lags fining upwards to laminated sandstones (field of the photograph about 1x2 m). B) Close-up on the sharp, erosional base of an orthoconglomerate lag (field of the photograph about 0.65x1 m). C) Sandstone laminae cross-cutting at angles exceeding 30° (shell – bottom centre – for scale is about 4 cm across). D) Large-scale trough cross-bedding in sandstone bars alternating with bioturbated siltstones (L.A. Ronchi's arm for scale). E) Climbing sets of asymmetrical current ripples and trough-cross lamination in mature sandstones (hammer for scale). A)-C) = Lithozone 2, Porto Ferro section; D) = Lithozone 3 (lB), Torre del Porticciolo; E) = Lithozone 4 (uB), Cala Viola.

10), along with their remarkable width (exceeding 10 m in one instance) and the absence of mudclasts, strongly suggests that the braided streams were not ephemeral.

Lithozone 3 = lB (45÷50 m-thick) consists of alternating intervals of grey-greenish sandstones and deep red, micaceous siltstones (mud/sand ratio = 2.5 at the scale of the whole lithozone). Sandstones, arranged in locally coarsening-upward beds, display rough parallel, low-angle and trough cross-lamination (Fig. 6d): asymmetrical current ripples, climbing ripples and convolute lamination are also widespread. Imbricated pebbles at the base of sandstone beds, as well as alignments of winnowed platy pebbles at their top, locally occur, and mudcracks are also reported (Cassinis et al. 1996). Pebbles, commonly not exceeding 4 cm in diameter, consist of ignimbrite, milky quartz and metamorphics; well-rounded sandstone pebbles up to 12 cm in diameter are exceptionally found. A delta plain to delta front environment is indicated, with mouth bar sands, deposited during flooding stages, cyclically prograding onto coastal marshes to lower shoreface mudrocks.

Lithozone 4 = uB (over 36 m-thick) starts with a conglomerate bank, very rich in milky quartz pebbles, 3.3 to 3.5 m-thick all over the study area (Fig. 2b). An overall fining-upward suc-

lithozone	*direction range (°N)*	*indicator*
4	030-059	trough cross-bedding
4	030-059	imbricated pebbles
4	060-089	cross-lamination
4	060-089	cross-lamination
4	060-089	high-angle parallel bedding
4	090-119	cross-lamination
4	090-119	cross-bedding
4	090-119	trough cross-bedding
4	090-119	trough cross-bedding
4	120-149	cross-lamination
4	120-149	trough cross-bedding
4	120-149	imbricated pebbles
4	150-179	trough cross-bedding
4	150-179	trough cross-bedding
4	180-209	trough cross-bedding
4	240-269	trough cross-bedding
4	240-269	high-angle parallel bedding
4	270-299	trough cross-bedding
4	300-329	trough cross-bedding
3	090-119	current ripples
3	120-149	trough cross-bedding
3	120-149	imbricated pebbles
2	060-089	imbricated pebbles
2	060-089	channel-lags
2	120-149	imbricated pebbles

Table 2. Palaeocurrent indicators from the mid-Permian to Triassic clastic succession of Nurra; Lithozones 2 to 4 as in Fig. 3.

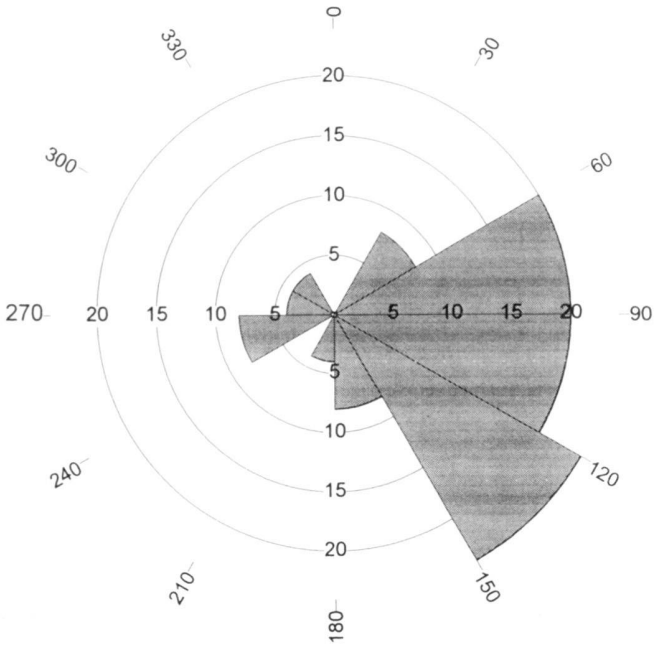

Fig. 7. Rose diagram for palaeocurrent directions in the Torre del Porticciolo area (Porto Ferro-Cala Viola section); mean ray at 114° N, mode at 120°÷150° N. Frequency percentages (5 to 25) are displayed along the four main axes.

cession follows, in which channelised lens-shaped beds, 10 to 30 cm-thick, of pebbly sandstones displaying imbricated pebbles and large-scale trough cross-bedding are overlain by pinkish coarse-grained sandstones exhibiting widespread high-angle and parallel to cross-lamination, as well as climbing sets of asymmetrical current ripples, clay plugs and oversized mudclasts (Fig. 6e). Coarsening-upward sandstone beds, more common in the middle part of the lithozone, display alignments of winnowed platy pebbles at their top and are again interpreted as the products of rising flood conditions; sparse pebbles, "drowned" in the sandstone matrix, also occur. Climbing ripples are especially common in the upper part of the lithozone, where they represent the sandy tail of fining-upwards cyclothems. Pebbles, up to 15 cm in diameter in the basal conglomerate bank but not exceeding 6 cm in the overlying beds, consist of milky quartz by far prevailing over ignimbrite. Lithozone 4 marks a new stage of fan progradation, after which distal braidplain to meandering river plain environments took over. The aeolian structures reported in Gasperi & Gelmini (1979) are questionable and can be also interpreted as fluviatile in origin.

At Monte Santa Giusta (15 metres exposed in the measured outcrop; 30÷40 metres reported in Gasperi & Gelmini 1979; about 50 metres reported in Carrillat et al. 1999), massive red paraconglomerates and poorly-sorted pebbly sandstones prevail, locally passing upwards to platy pebble lags and cross-laminated sandstones. A bluish-black sandstone layer, up to 1.6 m thick, is found 2.1 m below the base of the overlying transgressive dolomitic sandstones and hybrid carbonates. Pebbles consist of red ignimbrite (up to 20 cm in diameter), metamorphics (up to 15 cm) and milky quartz (up to 3.5 cm); rare sandstone pebbles up to 6 cm in diameter are also found. The described facies are consistent with an alluvial fan environment in which gravel and sand were deposited during ephemeral stream-floods.

Palaeocurrent indicators from Lithozones 2 to 4 (Tab. 2) document fluvial transport largely towards the ESE (mostly 60°÷150° N; Fig. 7), with a mean ray at 114° N and a mode at 120°÷150° N, corresponding to a prevailing southerly direction if Sardinia is restored to its Permian palaeoposition by a clockwise rotation of 50÷60° with respect to stable Europe (Zijderveld et al. 1970; Westphal et al. 1976). Abundance of reliable palaeocurrent indicators in the uB with respect to the structure-rich Lithozone 2 is due to spectacular three-dimensional exposures of the former unit at Cala Viola; Lithozone 2 is instead mostly two-dimensionally exposed along the flat cliff of Porto Ferro (Fig. 2a).

The subordinate antithetic palaeocurrent indicators in the uB (trough cross-bedding and high-angle parallel bedding) might be, at least in part, interpreted as backset beds. Alternatively, a tidal influence (Neri et al. 2000) would be consistent

with upper delta plain settings and with carbonate content increasing upsection in the uB. However, such an influence should have been subordinate because the red bed facies persists even in the upper part of the section, where plant debris and fresh-water crustaceans are found.

Heavy minerals analysis

Rationale

Although a time-consuming technique, heavy mineral (HM) analysis can provide useful information for sediment provenance, correlation of unfossiliferous clastic units, and distinction of drainage areas ("HM provinces"). In the following section, quantitative data on the HM suites of the upper part of the studied clastic succession are provided, bringing useful elements to support conclusions on the palaeogeographic reconstruction presented in this paper.

Materials and methods

Sandstone samples were mechanically crushed to granules not coarser than 4 mm in diameter ("pea size" of Folk 1974). Light particles finer than 62 μm were siphoned off (withdrawal at depth of 8 cm, 26 seconds after stirring); acid digest in nearly pure monochloroacetic acid (99%) and warm oxalic acid (N/10 = 4.6 g/l) in sonic tank, using metallic aluminium as catalyst, were alternated to washing in hydrogen peroxide and siphoning.

The resulting sand was sieved at the 500 and 250 μm meshes; HMs were separated in sodium metatungstate (density = 2.90), which masks the abundance estimates of detrital phyllosilicates whose density range straddles that of the heavy liquid (white micas = 2.80÷2.88, biotite = 2.70÷3.12 and chlorites = 2.50÷3.00), and that can thus settle down with the other HMs only when including high-density Fe-Ti aggregates.

HMs were mounted on microscope slides; at least 200 transparent detrital grains were counted on each slide following the line method (Galehouse 1971). Only in sample DSG 4, where the opaque minerals represent over 97% of the HM suite, all the 168 transparent grains on the slide were counted.

Mostly opaque grains from sample DSG 4 were mounted in thermosetting resin and analysed at both the WDS (kV = 15.0, nA ~ 300, livetime = 40÷80 seconds, natural amphibole and rhodonite as standards) and EDS (kV = 20.0, nA = 300÷350, livetime = 50 seconds, international standards and metallic cobalt for calibration) microprobes.

Heavy mineral suites

The low diagenetic grade of the studied succession resulted in the good preservation of the diverse HM suites, comprising metastable minerals sensitive to intrastratal dissolution (Morton 1985).

Zircon occurs in both fresh, commonly elongated, colourless, shiny-multifaceted euhedral crystals (Fig. 8a, b) and brownish, well-rounded to spherical and cigar-shaped grains (Fig. 8c). The former are likely to be first-cycle grains and might derive from penecontemporaneous acidic volcanics (Folk 1974), the latter are obviously polycyclic and sourced from older sedimentary to metasedimentary rocks. Rounded to well-rounded brownish grains, displaying pitted surfaces, are particularly abundant in sample DCV 5 and common in sample DCV 6 (Cala Viola section), whereas they are rare in the Monte Santa Giusta section.

Tourmalines mostly consist of deep green to brownish schorl and dravite, occurring as elongate prismatic grains with irregular fractured ends (Fig. 8d) and, less commonly, as basal or quasi-basal grains; their abundance in the Cala Viola section decreases upwards, although with low correlation coefficient and significance level ($r = -0.608$, sign. lev. > 10%). Blue indicolite and colourless achroite were also recorded.

Rutile mostly occurs as large, cigar-shaped grains ranging in colour from amber to deep red (Fig. 8e) to almost black; twinning and inclusions are widespread. Rutile is commonly derived from igneous and metamorphic rocks as well as from older sediments, and its authigenic origin cannot be ruled out.

Apatite, invariably colourless, commonly displaying dusty inclusions, occurs as both broken prismatic crystals and large, well-rounded grains (Fig. 8f).

Garnet occurs as angular, sharp-cornered, irregular colourless grains bounded by conchoidal fracture surfaces (Fig. 8o). *Spinel*, colourless and inconspicuous in the studied samples, was tentatively distinguished from garnet by its lower refractive index.

Chloritoid has been recognised with some uncertainty in the Monte Santa Giusta section and in the upper Cala Viola section: it occurs as platy, prismatic and angular irregular grains with very low birefringence on the basal plane.

Staurolite occurs as large, somewhat platy angular grains, commonly with conchoidal fractures, but occasionally preserving sharp edges and crystal faces; twinned crystals (Fig. 8l, m) are rare. It is abundant in the Monte Santa Giusta section, and present in low number in the Cala Viola section. Microprobe analyses on grains from sample DSG 4 (Monte Santa Giusta section) revealed a remarkably uniform composition (Tab. 3.2).

Epidote group, including zoisite and clinozoisite, comprises sharp angular ("bottleglass"), equidimensional (Fig. 8p) to elongate grains. They are abundant in the Monte Santa Giusta section, widespread but never exceeding 4.5% of the HM suite in the Cala Viola section. *Allanite* is easily discriminated from other epidotes by its deep colour and strong pleochroism.

Amphiboles, occurring as irregular fractured fragments to fibrous prismatic grains (Fig. 8h), are commonly greenish and belong to both the tremolite-actinolite and the hornblende series; rare bluish amphibole grains (Fig. 8i) may be identified as arfvedsonite because they display length-fast orientation and lack the distinctive pleochroism of the glaucophane-riebeckite series.

Clinopyroxenes include here both the augite and the diopside-hedenbergite groups, and *orthopyroxenes* both the hypersthene and the enstatite-ferrosilite groups. All pyroxenes occur as pale brown to greenish angular, fractured grains displaying etch-features ("hacksaw" terminations; Fig. 8n); strong pleochroism of brownish to bluish grains in sample DCV 11 suggests the occurrence of titanaugite to aegirinaugite. Pyroxenes, although deriving from a wide range of metamorphic and intermediate to basic magmatic rocks, are rare in recycled sediments due to their low chemical stability in the sedimentary environment; they are abundant in the Monte Santa Giusta section and in the upper Cala Viola section, starting from sample DCV 10.

Andalusite, rare and reported with some uncertainty, occurs as worn, moderately elongated prismatic grains with a turbid surface.

Monazite is common, although not abundant, in the Monte Santa Giusta section and in the upper Cala Viola section, starting from sample DCV 8. Small egg-shaped grains (Fig. 8j) derive from rounding of (100) tablets; pitted, abraded surfaces are common even in first-cycle grains due to the low hardness of the mineral.

Xenotime, occurring as subangular rectangular flakes of high relief and strong birefringence, has been tentatively discriminated from zircon by microscopical means alone; it seems to be inconspicuous in the studied samples.

Dumortierite, in unevenly terminated prismatic grains with conspicuous striations parallel to prism edges and distinctive pleochroism, was sporadically recorded in sample DSG 5.

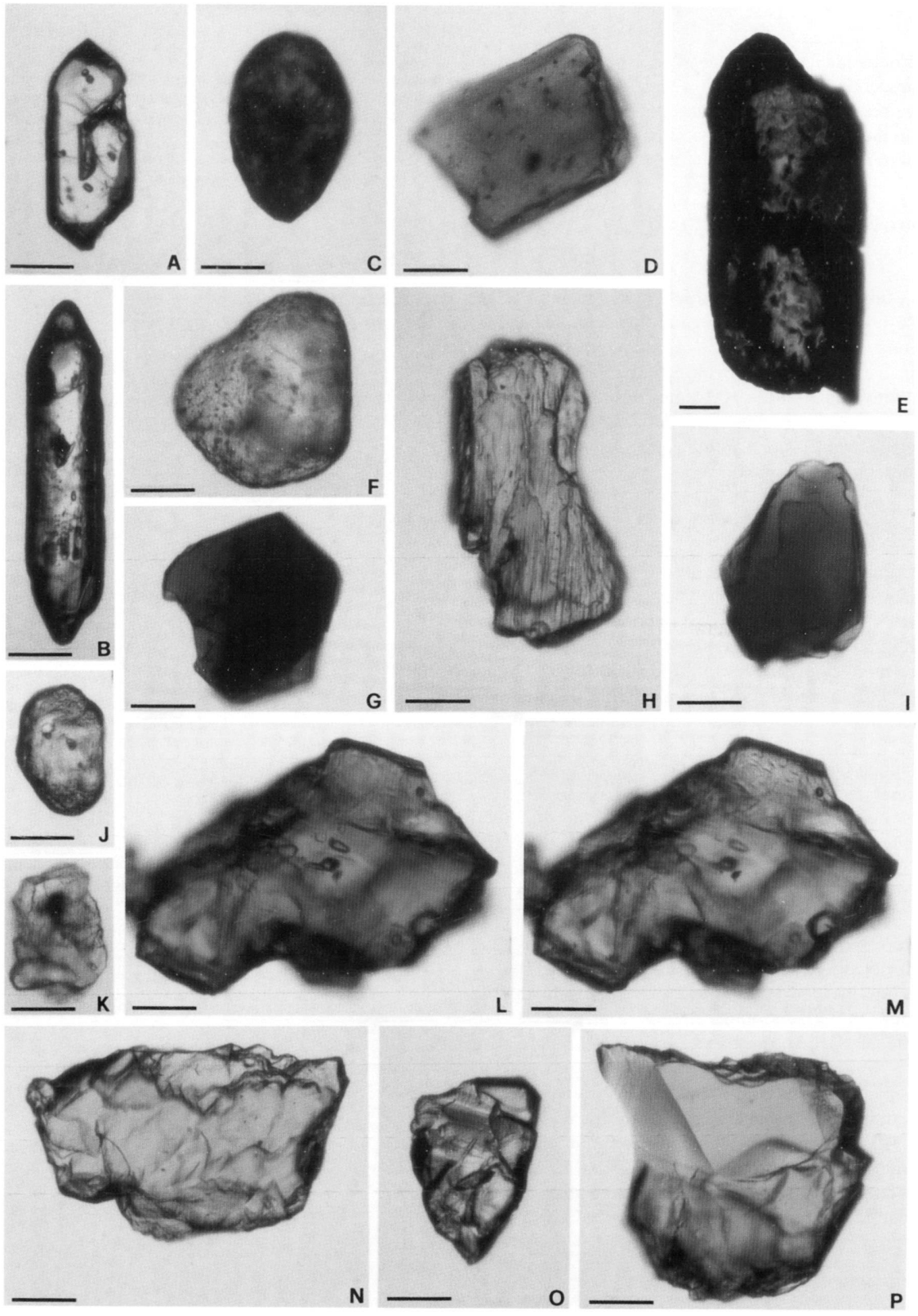

Fig. 8. Typical transparent heavy minerals from the studied suites. a, b) Elongate, euhedral, transparent zircon; c) subrounded brownish zircon; d) broken prismatic tourmaline; e) cigar-shaped, deep red rutile; f) rounded apatite; g) hexagonal flake of green biotite; h) fibrous prismatic amphibole (tremolite-actinolite series); i) angular irregular grain of bluish-green Na-amphibole; j) subrounded monazite; k) subangular, irregular crystal of authigenic baryte; l) angular, twinned staurolite with sharp crystal faces; m) same as l), rotated by 90°; n) angular orthopyroxene with dentate ends; o) angular irregular garnet with conchoidal fractures; p) angular equidimensional "bottleglass" epidote with sharp crystal faces. All photos are in plane polarised light; scale bar = 50 µm.

	1a	1b	1c	1d	2a	2b	2c
SiO_2	0,51	0,50	1,11	1,90	27,90	27,77	27,99
TiO_2	0,00	0,00	0,00	0,36	0,58	0,50	0,64
Al_2O_3	0,46	0,60	0,86	0,53	55,66	54,34	53,23
FeO_{tot}	0,00	0,00	2,20	0,39	13,11	14,28	13,54
MnO	59,13	58,41	54,97	52,12	0,53	0,41	0,34
CuO	1,97	2,54	2,48	1,82	0,00	0,00	-
MgO	0,35	0,54	0,45	0,29	1,11	0,99	1,53
CaO	0,80	0,88	0,91	0,56	0,00	0,00	0,01
BaO	11,98	10,58	9,13	9,63	0,00	0,00	-
Na_2O	2,77	2,86	3,05	3,16	0,00	0,00	0,00
K_2O	0,41	0,50	0,49	0,46	0,00	0,00	0,00
P_2O_5	0,00	0,00	0,00	0,00	0,00	0,23	-
Total	78,38	77,41	75,65	71,22	98,90	98,51	97,28

Table 3. Non-normalised EDS (1, 2a-b) and WDS (2c) analyses on single heavy minerals from sample DSG 4, Monte Santa Giusta section. 1 = authigenic Mn-oxide, best approaching the formula of Cu and Na-rich romanechite; 2 = detrital staurolite. Dashes indicate elements not detected; note remarkably uniform composition of detrital staurolites, pointing to a single nearby source.

Vesuvianite has been recognised with some uncertainty in the Monte Santa Giusta section and in the upper Cala Viola section (starting from sample DCV 9). It occurs as irregular to prismatic grains with anomalous interference colours.

Sphene, occurring as irregular, subangular grains, is common in both studied sections; as a detrital grain it derives from a variety of igneous and metamorphic rocks, but it can also be authigenic in sediments.

Anatase, in small rectangular grains of authigenic origin, was sporadically recorded. A single grain of *brookite*, squarish and striated, displaying incomplete extinction, was also found.

Detrital phyllosilicates include *biotite* (Fig. 8g), abundant only in sample DSG 5 (Monte Santa Giusta section) probably also as a consequence of an incomplete separation procedure, *muscovite* (including other optically indistinguishable white micas, e.g., paragonite), conspicuous in the studied sands before HM separation but rare in the heavy residues due to the marked cut-off effect exerted by the sodium metatungstate, and *chlorite*, recorded in both of the studied sections.

Transparent authigenic minerals include both *baryte*, occurring in irregular crystals to aggregates (Fig. 8k) and representing the dominant HM in the lower and middle parts of the Cala Viola section (up to 86% of the HM suite in sample DCV 7), and *dolomite*, in poorly formed and abraded rhomboedra, recorded only in sample DCV 9 (12% of the HM suite).

Opaque minerals in sample DSG 4 occur as irregular, powdery aggregates occupying an interstitial position in the sandstone and representing over 9% of rock volume (Ronchi 1993). Under observation by the SEM, clusters of platy to fibrous tiny crystals (Fig. 9) were also recognised. On microprobe analysis, such aggregates turned out to be invariably hydrous Mn-oxides, best fitting in the formula of romanechite $[(Ba, H_20)(Mn^{4+}, Mn^{3+})_7O_{10}$; Tab. 3.1]; however, since specific diffraction analyses have not been carried out, the occurrence of other wad minerals, such as cryptomelane, Ba-todorokite and vernadite, cannot be ruled out. All these authigenic oxides, interpreted as colloidal in origin, are reported to form in continental setting as a result of precipitation from manganogels during prolonged exposure of sediments to subaerial chemical weathering, under humid climatic conditions favourable to lateritisation (Dammer et al. 1996; Shvanov et al. 1998).

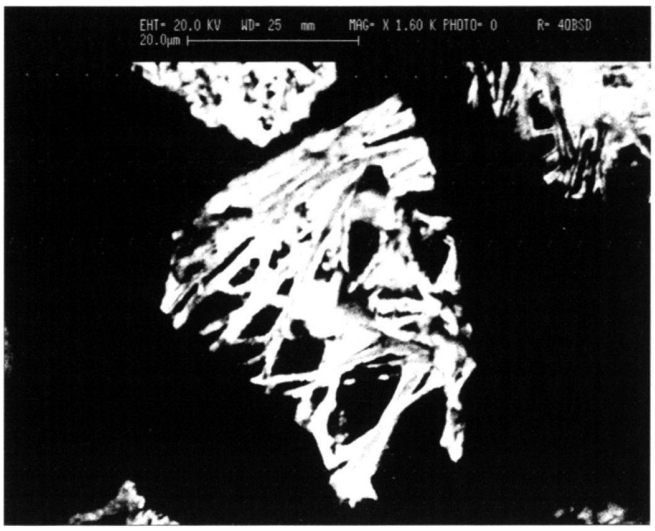

Fig. 9. Back-scatter SEM image of an aggregate of tiny flakes of authigenic hydrous Mn-oxides.

Discussion: heavy mineral provenance

The described HM suites document provenance from a geologically complex source area, including crystalline basement, volcanic and sedimentary rocks. Diverse lithologies are consistent with the indications provided by bulk modal data on sandstones: indeed, detrital modes mostly cluster in the "recycled orogen" field of Dickinson (1985). The Permian geological setting of Southern Europe fits in these constraints, because the source areas of the Hercynian range comprised the Variscan metamorphic basement, its post-Variscan intrusives and the volcanic and clastic successions deposited since the Late Westphalian.

In general, contribution from sedimentary successions is difficult to evaluate quantitatively. In the studied suites, well-rounded grains are rare and mostly consist of apatite and monazite, that is, low-hardness HMs: a notable exception is represented by the brownish zircons of the lower Cala Viola section (samples DCV 6-7). Since the ZTR index (Hubert 1962) is invariably higher in samples from the Torre del Porticciolo area than in samples from the Monte Santa Giusta area, recycled detritus can be inferred to be more abundant in the former.

Differences in the HM suites from the two outcrop areas are remarkable (Tab. 4; Fig. 10), allowing to identify a Torre del Porticciolo HM province as distinct from a Monte Santa Giusta HM province. Such differences in roughly coeval sections might be interpreted by either distinct source rocks and/or different environmental conditions before burial.

Although obtained on a small statistical database, correlation between the abundance of single HM species and textural parameters (grain size, sorting; Tab. 4) is generally poor. Only the abundance of garnet within the Monte Santa Giusta Province is correlated at significance level < 5% with grain size; correlation is however lost if the data from both provinces

Sample	DCV 5	DCV 6	DCV 7	DCV 8	DCV 9	DCV 10	DCV 11	DSG 1	DSG 2	DSG 3	DSG 4	DSG 5
Grain size (Φ)	0,65	1,25	1,00	1,25	2,00	2,00	2,25	1,25	2,00	0,75	0,25	-
Sorting	Mod	Mod	Mod-W	Mod-P	Mod	Mod	Mod	Mod-P	Mod-P	Poor	Mod-P	-
Zircon	26,0	24,5	32,0	49,3	34,0	26,5	25,5	10,0	5,0	7,5	2,4	13,3
Tourmalines	58,0	55,8	38,4	11,1	29,5	32,0	18,5	27,0	29,0	30,5	29,2	29,6
Rutile	1,5	5,3	5,9	15,5	11,5	9,5	17,5	3,5	12,0	7,5	2,4	15,3
Spinel	-	-	-	-	0,5	0,5	-	-	0,5	1,0	-	-
Chloritoid	-	-	-	0,5	1,0	-	-	1,5	2,5	-	1,8	2,9
Apatite	-	0,5	2,5	1,0	1,0	0,5	-	3,5	2,5	-	6,0	1,0
Garnet	0,5	-	-	1,0	1,5	-	-	1,0	3,5	1,5	-	2,0
Staurolite	0,5	tr.	1,0	tr.	3,0	0,5	0,5	12,5	5,0	11,0	12,5	6,9
Epidote	4,5	3,4	3,9	1,5	-	4,0	1,0	20,5	15,5	15,5	20,8	4,4
Allanite	1,5	1,4	-	-	-	5,0	3,5	1,5	tr.	2,5	1,2	2,9
Amphiboles	1,5	0,5	3,0	0,5	2,0	5,0	1,0	2,0	4,0	5,0	6,5	4,9
Andalusite	0,5	0,5	-	-	0,5	1,5	tr.	-	-	-	-	1,0
Clinopyroxenes	1,0	1,0	1,0	-	1,5	2,5	12,0	3,5	7,5	5,5	8,9	2,0
Orthopyroxenes	0,5	1,0	0,5	-	0,5	2,0	4,5	4,0	5,0	2,5	5,3	1,0
Monazite	1,5	-	-	2,5	0,5	1,5	4,5	5,5	1,0	1,5	-	2,9
Xenotime	-	-	-	0,5	-	-	0,5	-	-	-	-	0,5
Dumortierite	-	-	-	-	-	-	-	-	-	-	-	0,5
Vesuvianite	-	-	-	-	0,5	0,5	0,5	-	1,0	0,5	1,2	-
Sphene	2,0	6,2	11,8	16,4	12,5	8,5	10,5	4,0	6,0	8,0	1,8	8,9
Anatase	0,5	-	-	-	-	-	tr.	-	-	-	-	-
Brookite	-	-	-	0,5	-	-	-	-	-	-	-	-
Total	100,0	100,0	100,0	100,0	100,0	100,0	100,0	100,0	100,0	100,0	100,0	100,0
Transparent grains/Total	0,823	0,862	0,847	0,650	0,801	0,826	0,730	0,740	0,450	0,656	0,030	0,234
Detrital transp./Tot. Transp.	0,285	0,260	0,140	0,595	0,288	1,000	0,990	0,990	1,000	1,000	0,991	1,000
ZTR index	0,860	0,856	0,763	0,759	0,750	0,680	0,615	0,405	0,460	0,455	0,340	0,582

Table 4. Quantitative data on the heavy mineral suites of the studied sandstone samples obtained through line counting (but for sample DSG 4, counted by fields). Grain size and sorting data after Ronchi (1993); tr. = mineral species observed, although not counted. Sample DSG 5 was too loose to obtain a thin section, so textural data are lacking.

are plotted together, and in this case only the abundance of rutile is correlated to grain size at significance level < 5%, large and dense rutile crystals being enriched in coarser-grained sandstones, although with poor correlation coefficient (r = 0.754). Control by sorting over the abundance of staurolite (r = 0.734) and epidote (r = 0.723) and on the ZTR index (r = -0.726) is also indicated on the whole sample population at significance level < 5%, although with poor correlation coefficients; the first observation might suggest that both staurolite and epidote were derived from nearby local sources, whereas the second suggests an higher mineralogical stability of texturally more mature sediments, as already indicated by bulk sandstone composition vs. texture.

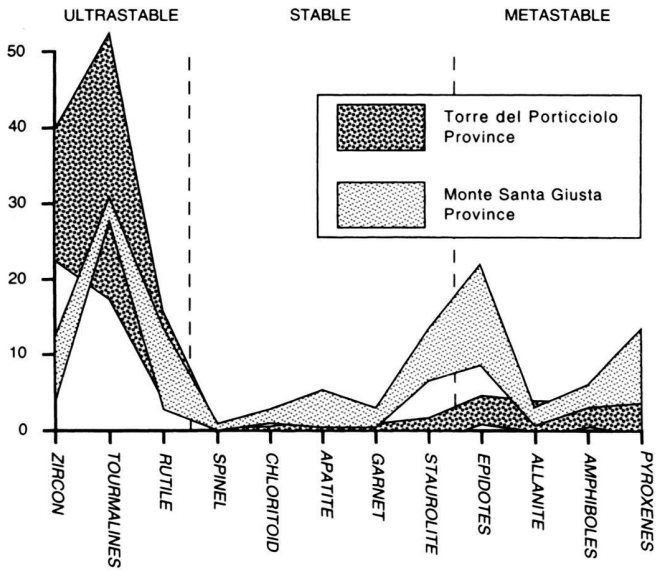

Fig. 10. Abundance of non-authigenic, transparent heavy minerals in the two recognised heavy minerals provinces; order of stability with respect to intrastratal dissolution under burial diagenesis after Morton (1985). Width of the ribbons is one standard deviation each side of the mean.

Thus, assuming that control by sedimentary processes on the abundance on the HMs in the two distinct provinces was not relevant, it must be concluded that, according to the available quantitative data, the two studied outcrop areas differ remarkably as to relative contributions from various source rock types.

In the Torre del Porticciolo province, composition of the HM suites is dominated by both "neovolcanic" and recycled zircon, along with tourmaline and rutile, and is therefore consistent with provenance from mostly volcanic and intrusive to metamorphic basement rocks, incorporating a significant amount of recycled detritus from older sediments. In the Monte Santa Giusta province, the HMs were derived essentially from low to medium-grade metamorphic (epidotes, staurolite, pyriboles) and intrusive (pyriboles, monazite) basement rocks, with minor contribution from volcanic and sedimentary successions. Two alternative explanations for the observed compositional differences might be:

1. the Monte Santa Giusta arkoses and the Torre del Porticciolo volcanic arenites to sublitharenites were deposited in separate basins. Due to reduced thickness and proximal facies of the studied successions, this inference would require a basement ridge acting as a divide between the basins, which does not agree with field and borehole data;

2. the Monte Santa Giusta arkoses were deposited by a local alluvial fan, flowing into the Torre del Porticciolo distal floodplain, which was fed by a larger and more complex drainage system, receiving detritus from distant northern sources. First-cycle detritus from basement source rocks, similar to those feeding the Monte Santa Giusta fan, would have been diluted by overwhelming quantities of volcanic detritus from the Permian volcanics (mostly represented by fresh euhedral zircon and apatite) and by polycyclic detritus from older sediments (brownish abraded zircon and, possibly, some tourmalines and rutile). Uniform geochemistry of detrital staurolite supports the model of provenance of the Monte Santa Giusta clastics from a single, local source.

In detail, mutual statistical correlations at sign. lev. < 5% between the abundance of single HM species all over the study area suggest that supplies from three end-member crystalline source rocks, such as acidic magmatic rocks (zircon-monazite-allanite), medium- to high-grade metasediments (rutile-garnet-sphene-zircon-spinel) and low- to medium-grade metamorphic and intermediate to basic magmatic rocks (tourmalines-amphiboles-chloritoid-staurolite-epidote-pyroxenes), varied with time. This simple model becomes more complicated by the variable input of ultrastable to stable grains recycled from older sedimentary successions.

The ZTR index decreases upsection in the Cala Viola Section (correlation coefficient of ZTR % vs. stratigraphy in metres = - 0.934, sign. lev. < 5%). This trend can hardly be explained by more severe diagenetic effects at depth (Morton 1985) because of the small differences in burial depth of the studied samples and the overall low diagenetic grade of the Permian to Lower Triassic clastics of Nurra. Therefore, decreasing ZTR index values can be interpreted as a provenance signal, recording increasing flux of first-cycle detritus from the progressive unroofing of basement lithologies, paralleled by decreasing contribution from both volcanics, providing fresh zircons, and older sediments shedding recycled grains. The latter are particularly well represented in the lowermost sample DCV 5, where zircons are dominantly rounded with pitted surfaces, and "neovolcanic" crystals are negligible.

The unroofing sequence model is consistent with increasing amounts of accessory minerals from acidic igneous rocks (monazite, apatite) from the middle part of the Cala Viola section (sample DCV 8), and then increasing proportions of pyroxenes from sample DCV 10.

It is noteworthy that a similar unroofing sequence is not recorded by sandstone detrital modes within the uB (Ronchi 1993), although it is evident at the scale of the whole Verrucano Sardo (Fig. 5).

Palaeogeographic implications

Palaeoclimate. Contrasting with views of a world-wide hot and arid climate throughout the Early Triassic (Dickins 1993) and the reef and evaporite-dominated Middle Triassic (Frakes 1979), data obtained from the Buntsandstein of Nurra support the hypothesis of a more humid climate – at least seasonally - during these epochs.

In fact, locally abundant authigenic hydrous Mn-oxides in possibly Lower Triassic to Anisian sandstones are likely to have formed as a result of sediment weathering in hot and humid climatic conditions favourable to lateritisation; moreover, sedimentary features and dimensions of the Permotriassic fluviatile channels suggest that they were seasonal to perennial rather than ephemeral. The ferroan interstitial minerals, widespread in continental red beds (Lithozones 2 and 4), provide a less conclusive evidence, but, after the long debate on the Walker vs. Van Houten models, are currently interpreted as reflecting seasonal rainfall in semiarid climates (Parrish 1993 and references therein). The local occurrence of *Equisetum* in Lithozone 4 does not point unambiguously to humid climates, as it might be expected by looking at present-day forms (R.H. Wagner, pers. comm.).

Global evidences for humid palaeoclimates in the Triassic have been sceptically rejected by some authors (e.g. Dickins 1993), but might be accounted for by a supposed Pangean megamonsoon (Parrish et al. 1982; Parrish 1993), causing high seasonal rainfall in coastal regions, extending to continental interiors not shielded by mountain ranges.

Lateritisation of continental sediments, as inferred by the observed Mn-rich weathering profiles, is consistent with 1) equatorial to tropical palaeolatitudes indicated for Sardinia at Early to early mid-Triassic times (Dercourt et al. 1993), 2) the high rainfall figures, increasing with steep gradients with respect to the arid central Europe, proposed for the western end of the Tethys Ocean in the Induan (Parrish et al. 1982), and 3) the areal distribution of favourable conditions (over 70% probability) for equatorial humid environs in the Early Triassic (Golonka et al. 1994).

Palaeogeography. The observed compositional differences between the two studied outcrop areas bear relevant implications on the palaeogeography of Nurra (Fig. 11). The Monte Santa Giusta alluvial fan is best ascribed to an ephemeral stage of clastic sedimentation over a basement high, exposed to erosion up to possibly Late Permian times, shortly before the Middle Triassic marine transgression. To the present-day south (corresponding to the Permian SW), the inferred basement high faced an articulated continental basin where alluvial fan environments had been progressively evolving to a vast floodplain facing a stream- to possibly tide-dominated delta. Even after the major marine transgression, possibly starting in the Illyrian at Punta del Lavatoio, but reliably documented only since the Ladinian at Monte Santa Giusta, the persistence of hybrid facies (silty to sandy vuggy dolostones, over 25 m-thick) in the Monte Santa Giusta area points to on-

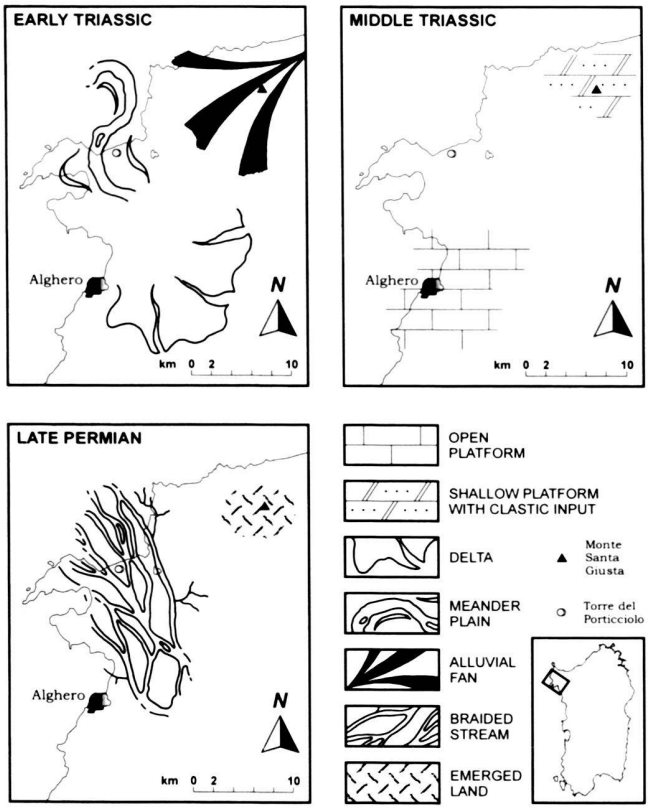

Fig. 11. Simplified palaeogeographic sketches for Nurra at Late Permian to Middle Triassic times; scarcity of biostratigraphic checkpoints does not allow to sharpen the time windows. Nurra is restored to its approximate Permian palaeoposition with respect to stable Europe by a clockwise rotation of 50° to 60° (Zijderveld et al. 1970; Westphal et al. 1976).

going erosion of nearby emerged sources (Fig. 11). The Permian-Anisian floodplain of the Torre del Porticciolo Province might thus have been flooded at earlier times, accommodating bioclastic and algal shallow shelfal limestones, while in the Monte Santa Giusta Permian swell intertidal carbonate-siliciclastic sediments were still being deposited (compare with the facies model of Carrillat et al. 1999).

Palaeocurrent indicators suggest a Permian to Early Triassic southerly transport for the alluvial sediments. This might be consistent with the occurrence of uplifted basement areas within the Hercynian range in the present-day central to southern France (Dercourt et al. 1993), where a dominantly southerly-directed fluvial system is often suggested during the post-Hercynian (J.-P. Deroin, pers. comm.). Some contrasting northward palaeocurrents, locally reported from the Lower Permian of the Toulon basin (Broutin et al. 1994), may fit in an early scenario of basin-and-swell palaeotopography, and are not uncommon even in present-day complex drainage systems.

Palaeogeodynamics. The investigated area is too small and the examined outcrops are too scattered to draw inferences of general value on the geodynamic scenario that controlled sedimentation: a wrench setting, causing prominent transtensional and subordinate transpressive displacements within the Hercynian megasuture, is commonly indicated for southern Europe in the Late Paleozoic (Arthaud & Matte 1977). Modal palaeocurrent indicators presented here (120°÷150° N), however, correspond well to the regional tectonic trends as documented by the major Cévennes (Languedoc), Nîmes (Provence) and Campidano (Sardinia) faults (Broutin et al. 1994), once restored to the Permian palaeoposition of Sardinia with respect to stable Europe. In this view, the inference of a Permian inheritance controlling the major Campidano trough (Gasperi & Gelmini 1979) gains support. During that time, according to modern and widely accepted palaeogeographic reconstructions, the Corso-Sardinian Block was adjacent to the western Southern Alps, where a similar wrench setting is convincingly documented (Massari 1986 and references therein). Actually, the Permian of Nurra is more similar to the Permian succession of the Southern Alps (Cassinis et al. 1988) than to the typical Germanic Permian: the Punta Lu Caparoni Formation is an equivalent, at much smaller scale, of the Collio Formation, and the Verrucano Sardo (in the sense here proposed) closely resembles the Verrucano Lombardo in terms of facies, bulk sandstone petrography and stratigraphic position (Sciunnach et al. 1996). Although the typical Buntsandstein facies is not represented anywhere in the Southern Alps, the progradation of alluvial fans at the base of the uB might have been enhanced by a "phase" of tectonic activity that is clearly documented to have occurred in the Southern Alps since the Olenekian and up to the Pelsonian (De Zanche & Farabegoli 1981; Sciunnach et al. 1996). The succession turned to a more typical Germanic facies only from the Ladinian–Carnian, while in the Southern Alps volcaniclastic facies – not reported anywhere in Sardinia – were being deposited. This may have represented a turning point in the evolution of Southern Europe, initiated by a major phase of plate rearrangement, preceding the Norian rifting and Liassic spreading of the Alpine Tethys (Bertotti et al. 1993 and references therein).

Acknowledgements

This paper relies on field observations, stratigraphic and sedimentologic data, and sandstone detrital modes, collected within the framework of the Tesi di Laurea work by L.A. Ronchi, tutored by M. Gaetani, E. Garzanti and the author. Heavy mineral separations were assisted by L. Trombino; WDS and SEM-EDS sessions by D. Biondelli and A. Rizzi respectively (grants by A. Gregnanin); photomicrograph sessions by R. Crespi. Useful discussions with J.-P. Deroin, E. Sciesa and R.H. Wagner are thankfully acknowledged. The paper benefited from constructive reviews by K.A.W. Crook, H. Friis, M. Gaetani, M. Mange, M. Vuagnat and G.G. Zuffa. Project MURST-1999 "L'eredità litosferica mesozoica tetidea nei processi subduttivi e collisionali del Mediterraneo centro-orientale".

REFERENCES

AIGNER, T. & BACHMANN, G.H. 1998: Sequence Stratigraphy of the Germanic Triassic: A Short Overview. In: Excursions of the International Symposium on the Epicontinental Triassic, Halle (Saale), Sept. 1998 (Ed. by BACHMANN, G.H., BEUTLER, G. & LERCHE, I.), Hallesches Jb. Geowiss. Reihe B 6, 23-26.

ARTHAUD, F. & MATTE, P. 1977: Late Paleozoic strike-slip faulting in southern Europe and northern Africa: result of a right-lateral shear zone between the Appalachians and the Urals. Geol. Soc. Am. Bull. 88, 1305–1320.

BERTOTTI, G., PICOTTI, V., BERNOULLI, D. & CASTELLARIN, A. 1993: From rifting to drifting : tectonic evolution of the South-Alpine upper crust from the Triassic to the Early Cretaceous. Sed. Geol. 86, 53–76.

BROUTIN, J., DOUBINGER, J., GISBERT, J. & SATTA-PASINI, S. 1988: Premières datations palynologiques dans le facies Buntsandstein des Pyrénées catalanes espagnoles. C.R. Acad. Sci. 301, 159–163.

BROUTIN, J., CABANIS, B., CHÂTEAUNEUF, J.-J. & DEROIN, J.-P. 1994: Evolution biostratigraphique, magmatique et tectonique du domaine paléotéthysien occidental (SW de l'Europe): implications paléogéographiques au Permien inférieur. Bull. Soc. géol. France 165(2), 163–179.

BROUTIN, J., CASSINIS, G., CORTESOGNO, L., GAGGERO, L., RONCHI A. & SARRIA, E. 1996: Research in progress on the Permian deposits of Sardinia (Italy). Permophiles 28, 45–48.

CARRILLAT, A., MARTINI, R., ZANINETTI, L., CIRILLI, S., GANDIN, A. & VRIELYNCK, B. 1999: The Muschelkalk (Middle to Upper Triassic) of the Monte di Santa Giusta (NW Sardinia): sedimentology and biostratigraphy. Ecl. geol. Helv. 92, 81–97.

CASSINIS, G., MASSARI, F., NERI, C. & VENTURINI, C. 1988: The Continental Permian in the Southern Alps (Italy). A Review. Z. geol. Wiss. 16(11–12), 1117–1126.

CASSINIS, G., CORTESOGNO, L., GAGGERO, L., RONCHI, L.A. & VALLONI, R. 1996: Stratigraphic and petrographic investigations into the Permian-Triassic continental sequences of Nurra (NW Sardinia). Cuad. Geol. Iber. 21, 149–169.

DAMMER, D., CHIVAS, A.R. & MCDOUGALL, I. 1996: Isotopic dating of supergene manganese oxides from the Groote Eylandt deposit, Northern Territory, Australia. Econ. Geol. 91(2), 386–401.

DERCOURT, J., RICOU, L.-E. & VRIELYNCK, B. 1993: Atlas Tethys Palaeoenvironmental Maps. Gauthier-Villars, Paris.

DE STEFANI, G. 1891: Cenni preliminari sui terreni mesozoici della Sardegna. Atti Acc. Naz. Lincei, Rend. Cl. Sc. Fis. Mat. Nat. 7, 427–431.

DE ZANCHE, V. & FARABEGOLI, E. 1981: Scythian tectonics in the Southern Alps: Recoaro phase. Geol. Pal. Mitt. Inn. 10(10), 289–304.

DICKINS, J.M. 1993: Climate of the Late Devonian to Triassic. Palaeogeogr. Palaeoclim. Palaeoecol. 100, 89–94.

DICKINSON, W.R. 1970: Interpreting detrital modes of graywacke and arkose. J. Sed. Petr. 40, 695–707.

DICKINSON, W.R. 1985: Interpreting provenance relations from detrital modes of sandstones. In: Provenance of arenites (Ed. by ZUFFA, G.G.), NATO-ASI Series, Reidel, Dordrecht, 333–361.

DICKINSON, W.R. & RICH, E.I. 1972: Petrologic intervals and petrofacies in the Great Valley Sequence, Sacramento Valley, California. Geol. Soc. Am. Bull. 83, 3007–3024.

FOLK, R.L. 1974: Petrology of sedimentary rocks. Hemphill's, Austin, 1–182.

FONTANA, D., GELMINI, R. & LOMBARDI, G. 1982: Le successioni sedimentarie e vulcaniche carbonifere e permo-triassiche della Sardegna. In: Guida alla Geologia del Paleozoico sardo. Guide Geol. Reg. Soc. Geol. It., 183–192.

FRAKES, L.A. 1979: Climates throughout Geologic Time. Elsevier, Amsterdam, 1–310.

FRANCESCHELLI, M., MEMMI, I. & RICCI, C.A. 1982: Zoneografia metamorfica della Sardegna settentrionale. In: Guida alla Geologia del Paleozoico sardo. Guide Geol. Reg. Soc. Geol. It., 137–149.

GALEHOUSE, J.S. 1971: Point counting. In: Procedures in Sedimentary Petrology (Ed. by CARVER, R.E.), John Wiley, New York, 385–407.

GANDIN, A. 1978: Il Trias Medio di Punta del Lavatoio (Alghero, Sardegna NW). Mem. Soc. Geol. It. 18, 3–13.

GASPERI, G. & GELMINI, R. 1979: Il Verrucano della Nurra (Sardegna nord-occidentale). Mem. Soc. Geol. It. 20, 215–231.

GHEZZO, C. & ORSINI, J.B. 1982: Lineamenti strutturali e composizionali del batolite ercinico sardo-corso in Sardegna. In: Guida alla Geologia del Paleozoico sardo. Guide Geol. Reg. Soc. Geol. It., 165–181.

GOLONKA, J., ROSS, M.I. & SCOTESE, C.R. 1994: Phanerozoic paleogeographic and paleoclimatic modeling maps. In: Pangea: global environments and resources (Ed. by EMBRY, A.F., BEAUCHAMP, B. & GLASS, D.J.), Can. Soc. Petr. Geol. 17, 1–47.

HAQ, B.U., HARDENBOL, J. & VAIL, P.R. 1987: The chronology of fluctuating sea level since the Triassic. Science 235, 1156–1167.

HOLSER, W.T. & MAGARITZ, M. 1987: Events near the Permian-Triassic boundary. Mod. Geol. 11, 155–180.

HUBERT, J.F. 1962: A zircon-tourmaline-rutile maturity index and the interdependence of the composition of heavy mineral assemblages with the gross composition and texture of sediments. J. Sed. Petr. 32, 440–450.

KOSSOVSKAYA, A.G. & SHUTOV, V.D. 1970: Main aspects of the epigenesis problem. Sedimentology 15, 11–40.

LOTTI, B. 1931: Relazione generale riassuntiva dei tre sondaggi per la ricerca del carbone paleozoico nei piani di Alghero. Boll. R. Uff. Geol. It. 56(4), 1–6.

LOVISATO, D. 1884: Nota sopra il Permiano ed il Triassico della Nurra in Sardegna. Boll. Com. Geol. It. 15, 305–324.

MASSARI, F. 1986: Some thoughts on the Permo-Triassic evolution of the South-Alpine area. Mem. Soc. Geol. It. 34, 179–188.

MORTON, A.C. 1985: Heavy minerals in provenance studies. In: Provenance of arenites (Ed. by ZUFFA, G.G.), NATO-ASI Series, Reidel, Dordrecht, 249–277.

NERI, C., RONCHI, A., CASSINIS, G., FONTANA, D. & STEFANI, C. 2000: The Permian-Triassic succession of Cala Viola-Porto Ferro. Stratigraphy, sedimentology and sandstone petrography. The Continental Permian Int. Congr. Field Trip Guidebook, 102–105.

PARRISH, J.T. 1993: Climate of the Supercontinent Pangea. J. Geol. 101, 215–233.

PARRISH, J.T., ZIEGLER, A.M. & SCOTESE, C.R. 1982: Rainfall patterns and the distribution of coals and evaporites in the Mesozoic and Cenozoic. Palaeogeogr. Palaeoclim. Palaeoecol. 40, 67–101.

PECORINI, G. 1962: Nuove osservazioni sul Permico della Nurra (Sardegna nord-occidentale). Atti Acc. Naz. Lincei, Rend. Cl. Sc. Fis. Mat. Nat. 32, 377–380.

PITTAU DEMELIA, P. & FLAVIANI, A. 1982: Aspects of the palynostratigraphy of the Triassic Sardinian sequences (preliminary report). Rev. Palaeobot. Palynol. 37, 329–343.

RONCHI, L.A. 1993: Stratigrafia del Permo-Trias della Nurra (Sardegna NW). *Tesi di Laurea, Università di Milano.*

RONCHI, A., BROUTIN, J., DIEZ, J.-B., FREYTET, P., GALTIER, J. & LETHIERS, F. 1998: New paleontological discoveries in some Early Permian sequences of Sardinia. Biostratigraphic and paleogeographic implications. C.R. Acad. Sci. 327, 713–719.

SCHMIDT, V. & MCDONALD, D.A. 1979: The role of secondary porosity in the course of sandstone diagenesis. SEPM Spec. Publ. 26, 175–207.

SCIUNNACH, D., GARZANTI, E. & CONFALONIERI, M.P. 1996: Stratigraphy and petrography of Upper Permian to Anisian terrigenous wedges (Verrucano Lombardo, Servino and Bellano Formations; western Southern Alps). Riv. It. Pal. Strat. 102, 27–48.

SHVANOV, V.N., FLOROV, V.T., SERGEEVA, E.I. et alii 1998: Sistematika i klassifikatsii osadochnykh porod i ikh analogov. Nedra, Saint-Petersburg, 1–352.

SOPEÑA, A., LOPEZ, J., ARCHE, A., PÉREZ-ARLUCEA, M., RAMOS, A., VIRGILI, C. & HERNANDO, S. 1988: Permian and Triassic rift basins of the Iberian peninsula. In: Triassic-Jurassic rifting. Continental breakup and the origin of the Atlantic Ocean and passive margins, part B (Ed. by MANSPEIZER, W.), Devel. in Geotect. 22, 757–786.

VARDABASSO, S. 1966: Il Verrucano sardo. Proceedings of the "Symposium sul Verrucano", Soc. Tosc. Sc. Nat., 293–310.

WESTPHAL, M., ORSINI, J. & VELLUTINI, P. 1976: Le microcontinent corso-sarde, sa position initiale: données paléomagnétiques et raccords géologiques. Tectonophysics 30, 141–157.

ZIJDERVELD, J.D.A., DE JONG, K.A. & VAN DER VOO, R. 1970: Rotation of Sardinia: palaeomagnetic evidence from Permian rocks. Nature 226, 933–934.

Manuscript received July 31, 2000
Révision accepted April 14, 2001